



ELSEVIER

Available online at www.sciencedirect.com

SCIENCE @ DIRECT®

Journal of Volcanology and Geothermal Research 149 (2006) 85–102

Journal of volcanology
and geothermal research

www.elsevier.com/locate/jvolgeores

Gas percolation in upper-crustal silicic crystal mushes as a mechanism for upward heat advection and rejuvenation of near-solidus magma bodies

Olivier Bachmann*, George W. Bergantz

Department of Earth and Space Sciences, University of Washington, Box 351310, Seattle, WA 98195-1310, USA

Received 10 December 2004; received in revised form 30 May 2005; accepted 16 June 2005

Abstract

Several crystal-rich, intermediate to silicic magmas erupted at arc volcanoes record a reheating event shortly prior to eruption: they provide evidence for remobilization of crystal mushes by mafic magmas. As hybridization between the mush and the mafic magma is often limited, bulk mixing could not be the dominant process in transferring heat. Conductive heating from a basaltic underplate plays a role, but a few characteristics of these rejuvenated mushes suggest that reheating occurs faster than predicted by conduction.

In the upper crust, a process that can transport heat faster than conduction, and still remain chemically nearly imperceptible, is the upward migration of a hot volatile phase (“gas sparging”) that originates in underplated mafic magmas. Using numerical simulations, we quantified the thermal effects of two-phase flow (a silicic melt phase and a H₂O–CO₂ fluid phase) in the pore space of shallow silicic mushes that have reached their rheological lock-up point (i.e., rigid porous medium, crystallinity ≥ 50 vol.%). Results show that the reheating rates are significantly faster than conduction for volatile fluxes $>0.1 \text{ m}^3/\text{m}^2 \text{ yr}$. Considering that volatiles can be rapidly exsolved from the underplated mafic magma, these high fluxes can be promptly reached, leading to fast reheating; sill-like batches of mushes with volumes similar to the 1995–present eruption of the Soufrière Hills (Montserrat, W.I.) can be reheated by a few tens of degrees and remobilized within days to weeks. At these high fluxes, a considerable volume of volatiles is needed (similar to the volume of mush being reheated). Large silicic systems ($>100\text{--}1000 \text{ km}^3$) require unrealistic amounts of volatiles to be reheated in a continuous, high-flux sparging event. Rejuvenation of batholithic mushes therefore requires multiple sparging episodes separated by periods dominated by near-conductive heat transfer at low-flux sparging ($<0.1 \text{ m}^3/\text{m}^2 \text{ yr}$) and may take up to 100–200 ky.

© 2005 Elsevier B.V. All rights reserved.

Keywords: silicic magma chamber; thermal modeling; gas phase; crystal mush; rejuvenation

* Corresponding author. Now at Section des Sciences de la Terre de l'Université de Genève, 13, rue des Maraichers, 1205 GENEVE, Switzerland.

E-mail addresses: olivier.bachmann@terre.unige.ch (O. Bachmann), bergantz@u.washington.edu (G.W. Bergantz).

1. Introduction

A deeply rooted assumption in the study of magmatic processes is that magmas move and differentiate largely as crystal-poor liquids and are the products of evolution linked to monotonic cooling prior to eruption. Yet, studies of crystal-rich volcanic units ranging in size from $<1 \text{ km}^3$ to $>1000 \text{ km}^3$ have shown evidence that supports an alternative to this prevailing model: magmas can crystallize to a rigid (but not completely solid) crystal mush and be reheated and partially remelted prior to eruption. Examples of thermally rejuvenated and remobilized crystal mushes include the recent and thoroughly monitored intermediate to silicic eruptions at the Soufrière Hills on the island of Montserrat (see references in *Geophysical Research Letters*, vol. 25, no. 18 and 19 (S.R. Young et al., eds.), the *Geological Society of London Memoir* 21 (T.H. Druitt and B.P. Kokelaar, eds.) and the 2003 issue 44 of *Journal of Petrology*), Mt. Unzen (e.g., Nakamura, 1995), and Mt. Pinatubo (e.g., Pallister et al., 1992), but also larger volcanic units such as the $\sim 100 \text{ km}^3$ Kos Plateau Tuff, a quaternary rhyolitic ignimbrite from the Aegean arc (Keller, 1969; Allen, 2001), and the 5000 km^3 Fish Canyon Tuff, one of the most voluminous pyroclastic units of the volcanic record (Lipman et al., 1997; Bachmann et al., 2002). These systems all share the following characteristics: (1) a high crystal content ($>35\text{--}40$ vol.% crystals); (2) a near-solidus mineral assemblage; (3) a high-SiO₂ rhyolite interstitial melt; (4) the absence of systematic compositional and thermal gradients; (5) ≤ 1 vol.% mafic enclaves; and (6) complex textures and mineral zoning, indicative of a protracted crystallization history and precarious equilibrium before eruption (in particular, partial remelting affecting largely the anhydrous mineral phases, as hydrous, mafic minerals often continue to grow during the reheating event).

The occurrence of mafic enclaves in the magmas suggests that rejuvenation and remobilization was triggered by the injection of hotter, more mafic magma at the base of the silicic mush in the upper crust. However, little hybridization occurred between the two magma bodies: their interaction was largely limited to heat transfer (Murphy et al., 2000; Couch et al., 2001; Bachmann et al., 2002; Devine et al., 2003; Rutherford and Devine, 2003). This important obser-

vation rules out magma mixing as the dominant heat transfer mechanism, and begs the question on how heat was added to the silicic magma. Conduction definitively played a role, but at least two observations suggest that some heat can be transported faster than conduction: (1) the eruption of extremely voluminous units ($>1000 \text{ km}^3$) of rejuvenated magma, such as the Fish Canyon Tuff (reheating such volumes by conduction, even by $50 \text{ }^\circ\text{C}$, would take a few millions of years); and (2) fast reheating rates estimated by diffusional profiles in Fe-Ti oxides of the Soufrière Hills andesite. Therefore, if some heat advection takes place in these rejuvenated systems, how could heat be transported with limited mass transfer?

One possibility, proposed by Couch et al. (2001), is that thermal convection occurs in the silicic magma body as a result of heating from below and destabilization of the hot boundary layer at the contact with the hot mafic magma (i.e., Rayleigh–Taylor instabilities). However, many of the rejuvenated magmas are very crystal-rich (>45 vol.% crystals) despite the fact that they display some remelting of their crystalline material, suggesting that they might have reached their rheological lock-up point (~ 50 vol.% crystal; Vigneresse et al., 1996; Petford, 2003). If crystals form a rigid skeleton, system-wide convection is impeded and another heat transfer mechanism is required.

On the basis of (1) the predicted occurrence of a low-density, low-viscosity fluid phase in shallow, volatile-rich magma chambers (e.g., Wallace et al., 1995; Stix and Layne, 1996; Lowenstern, 2000; Schmitt, 2001; Wallace, 2001); (2) isotopic evidence for the addition and transfer of a mafic volatile phase in silicic magmas (Gauthier and Condomines, 1999; Pichavant et al., 2002; Shimizu et al., 2005); and (3) petrological evidence for high volatile content during magma rejuvenation (Bachmann et al., 2002, 2005; Hammer and Rutherford, 2003), upward heat advection induced by volatile release from an underplated mafic magma (“gas sparging”) appears as a potentially viable physical mechanism for the rejuvenation of silicic mushes. This paper expands the work reported in a previous publication (Bachmann and Bergantz, 2003), developing this hypothesis in a more formal transport model. To illustrate the results, the “gas sparging” model will be evaluated in light of two natural examples with vastly different volumes for which we have abundant data: (a) the Fish Canyon

Tuff ($>5000 \text{ km}^3$; Lipman et al., 1997; Bachmann et al., 2002), and (b) the 1995-to-present eruption of the Soufrière Hills volcano, (Montserrat, W.I.; $<0.5 \text{ km}^3$; e.g., Sparks et al., 1998).

2. A schematic representation of upper-crustal magma reservoirs

Combining evidence from multiple sources (field and textural studies, geochemistry, geophysics), a potential picture of an upper-crustal “magma chamber” (at least in arc settings) can be portrayed (e.g., Koyaguchi and Kaneko, 2000; Bachmann and Bergantz, 2004; Hildreth, 2004; Fig. 1). Here are two fundamental assumptions that are critical to this study:

(a) Magmas are stored as mushes (crystallinity close to or above the rheological locking point of crystal–melt mixtures; $\geq 50 \text{ vol.}\%$) for most of their supra-solidus lifetimes (e.g., Marsh, 1996; Koyaguchi and Kaneko, 1999; Koyaguchi and Kaneko, 2000; Marsh, 2002; Hildreth, 2004). Evidence for a high crystallinity in silicic magmas stored in the upper crust include: (1) results from seismic tomography of “hot zones” beneath active silicic magmatic provinces, which reveal magma bodies with crystallinities above $50 \text{ vol.}\%$ (Dawson et al., 1990; Weiland et al., 1995; Steck et al., 1998; Miller and Smith, 1999; Zandt et al., 2003); and (2) high crystallinities (average of $25 \text{ vol.}\%$; Ewart, 1982) in most intermediate to silicic volcanic rocks in arcs, keeping

in mind that erupted rocks sample the least viscous, and thus the most crystal-poor material stored in the chamber.

(b) Most magmas in arcs are saturated with a fluid phase. The high initial volatile content of the magmas, their high crystallinity (crystal assemblage dominated by anhydrous phases) and the relatively shallow depth at which they reside ($1\text{--}4 \text{ kb}$) often combine to reach the saturation pressure of CO_2 and H_2O , triggering the exsolution of a low-density, low-viscosity volatile phase (e.g., Wallace et al., 1995; Lowenstern, 2000). Evidence for the presence of an exsolved volatile phase in these magmas include: (1) quantities of sulfur ejected during explosive volcanic eruptions in excess of the amount that can be dissolved in the magma, requiring the presence of a S-rich fluid phase in the chamber (e.g., Wallace et al., 1995; Wallace, 2001); (2) evidence from melt inclusions that crystallization in silicic magmas can occur in a gas-saturated environment (Wallace et al., 1999); and (3) the observation of increasing seismicity and surface doming in magmatic provinces following large tectonic earthquakes. These effects have been linked to rising bubbles in magma chambers (Linde et al., 1994).

2.1. Physics of gas transfer at the interface between stably stratified magmas

The mechanisms by which bubbles may (or may not) transfer from a mafic, volatile-saturated magma to an overlying, more evolved magma have been

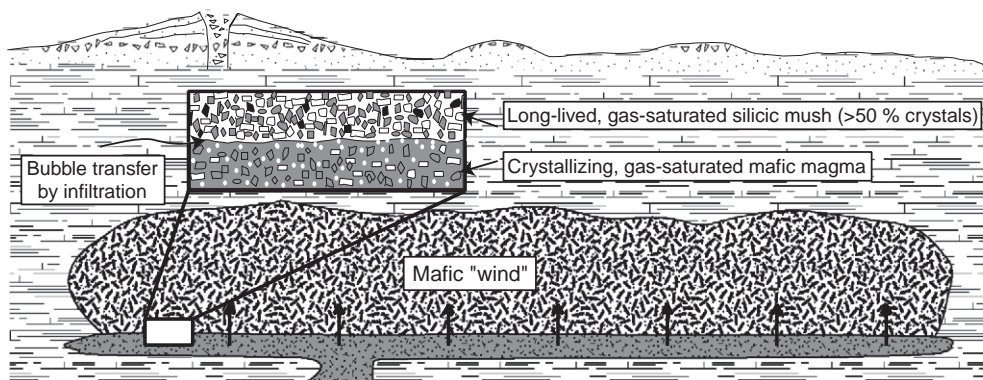


Fig. 1. Schematic diagram of the gas sparging hypothesis. The white rectangle is a blow-up of the interface between the two magmas, and mafic “wind” refers to the actual process of gas sparging; transfer of hot gas from a mafic intrusion underplating the silicic mush.

explored by Thomas et al. (1993); Cardoso and Woods (1999), and Phillips and Woods (2002). This recent work has been motivated by the early studies of Eichelberger (1980) and Huppert et al. (1982) on the potential importance of volatiles in inducing magma mixing. Using analog experiments and scaling laws, Phillips and Woods (2002) have proposed two consequences following the vesiculation of bubbles in the underlying, initially denser mafic magma: (1) if sufficient bubbles remain in suspension, the bulk density of the mafic magma may fall below the density of the overlying silicic magma, inducing large-scale overturn and thorough mixing (see also Bergantz and Breidenthal, 2001); and (2) if conditions are such that bubbles can rise and form a foam at the magma interface (e.g., low enough viscosity in the mafic magma, slow cooling rate), large-scale overturn may be suppressed and bubbles may rise in the overlying magma by infiltration or small bubble-rich plumes, carrying with them small amounts of mafic components. Clearly, in the model envisaged in the present study (mafic magma underplating a static, rigid, volatile-saturated silicic mush), large-scale overturn is highly unlikely, and gas is assumed to cross the interface by infiltration or small clusters of bubbles, with minor amounts of entrained mafic components. This is consistent with the geological observations in the rejuvenated systems mentioned above (significant heat, but limited mass transfer).

3. Description of physical model and algorithm

The numerical simulations performed in this study used a version of STOMP, an acronym for Subsurface Transport Over Multiple Phases (White and Oostrom, 2000). The STOMP simulator was initially designed to produce numerical predictions of thermal and multiphase flow in soils and groundwater at arid sites. It has been verified by comparison to analytical solutions, and validated against germane numerical, laboratory and field experiments (White and Oostrom, 2000). For the purpose of this study, the code was modified to account for characteristics of magmatic systems.

Our modeling was designed to address the multiphase flow and enthalpy advection resulting from the upward percolation of a buoyant fluid phase and a

silicate melt phase in the pore space of a rigid mush coupled with heat conduction from the hot lower boundary. In the computational domain, three phases were distinguished: (1) solid particles (crystals), which can actually consist of several (up to 11) different mineral phases; (2) a high-viscosity silicate melt; and (3) a gas (or “fluid”) phase (mixture of H₂O and CO₂). The following assumptions made for each phase (see Table 1 for symbols and Tables 2–4 for values used in the simulations):

(1) Crystal framework: ρ , C_p , κ and porosity (ϕ) were assumed constant in the chosen range of P – T conditions (600–1000 °C and 100 to 400 MPa; Murase and McBirney, 1973; Dobran, 2001). It was considered static and rigid. In reality, due to the density difference between the crystals (≥ 2600 kg/m³) and the interstitial high-SiO₂ melt (~ 2200 kg/m³), these porous framework have the tendency to progres-

Table 1
Symbols and constants

a	Grain size (m)
C_p	Specific heat (J/kg K)
g	Acceleration of gravity (9.81 m/s ²)
H	Thickness of porous medium (m)
κ	Thermal conductivity (W/m K)
k_ϕ	Total permeability (m ²)
k_r	Relative permeability (m ²)
K	Constant in Eq. (6) (50–200)
L	Latent heat (J/kg)
m	Mass (kg)
P	Pressure (Pa)
T	Temperature (°C), T_i =initial T , T_f =final T
V	Volume (m ³)
V_D	Darcy velocity (or volumetric flux per unit area; m ³ /m ² yr)
V_{Dgmax}	Maximum Darcy velocity for the gas phase (m ³ /m ² yr)
V_p	Seepage velocity (m/yr)
S	Surface of porous medium (m ²)
s	Relative saturation
t	Time (s)
z	Vertical direction (m)
α	Thermal diffusivity (m ² /s)
α_{vg}, m, n	van Genuchten parameters
β	Thermal expansion (1/K)
δ	Thickness of boundary layer (m)
κ	Thermal conductivity (W/m K)
μ	Viscosity (Pa s)
ϕ	Porosity
ρ	Density (kg/m ³)
χ	Proportion of phase change

Table 2
Material properties for the silicate melt (wetting phase)

Parameter	Value or range	Source
Thermal expansion (β ; 1/K)	0.00005	(Dobran, 2001)
Thermal conductivity (κ ; W/m K)	2	(Dobran, 2001)
Specific heat (C_p ; J/kg K)	1260	(Dobran, 2001)
Thermal diffusivity (α ; m ² /s)	0.000001	$\alpha = \kappa / (\rho C_p)$
Density (ρ ; kg/m ³) @ 800 °C	2270	Density of Fish Canyon interstitial melt (Whitney and Stormer, 1985)
Viscosity (μ ; Pa s)	$10^{4.5} - 10^{5.5}$	(Scaillet et al., 1998)
Surface tension (σ ; mN/m) between silicic melt and a fluid phase	85	For haplogranitic melt @ 800 °C (Bagdassarov et al., 2000)

Melt considered incompressible, Newtonian. C_p , β , κ , μ assumed constant in the chosen P – T range (600–1000 °C and 100–400 MPa).

sively “compact”, reducing porosity (and therefore permeability) in the lower part of the system. We have shown elsewhere (Bachmann and Bergantz, 2004) that melt flow rates in compacting silicic mushes are on the order of 10^{-9} – 10^{-10} m/s. By comparing these velocities with pore velocities of gas bubbles ($>10^{-9}$ m/s; calculated using the pore or seepage velocity (V_p), obtained by dividing the Darcy velocity (V_D) by the porosity and gas phase saturation: $V_p = V_D / (\phi(1-s_m))$), we can assume that porosity reduction due to compaction at the base of the mush is at least an order of magnitude slower and will not impede gas sparging. On the contrary, the occurrence of compaction might actually increase the reheating rate, as (1) the compacting volume, at the base of the mush, is closer to the heat source and can experience more remelting than shallower zones, which will counteract porosity reduction due to compaction; and (2) it will contribute to upward flow in the pore space.

(2) Silicate melt phase: μ , C_p , β , and κ were considered constant in the chosen range of P – T conditions. The melt was assumed incompressible and Newtonian. ρ was considered temperature-dependant, and was varied using the Boussinesq approximation (e.g., Philpotts, 1990: $\rho_f = \rho_i(1 - \beta(T_f - T_i))$), where ρ_f is the density at T_f , ρ_i the density at T_i , and β the thermal expansion (Table 2).

(3) Gas phase: All physical parameters were calculated assuming ideal mixing of H₂O and CO₂; μ ,

C_p , and κ were assumed constant in the chosen P – T range. ρ was calculated using the molar ratios of H₂O–CO₂ and the densities of pure H₂O and CO₂ provided by the National Institute of Standards and Technology webpage (NIST; <http://webbook.nist.gov/chemistry/fluid/>; Lemmon et al., 2003) for the pressure and temperature of interest. These values, which show a roughly linear dependence in pressure and temperature for the range of interest (small non-linearities produce kinks in the reheating curves; see Results section), were tabulated and updated during the simulation. The molar ratio in the gas phase was chosen to vary between 0.2 and 0.5 (volatile-rich mafic magmas generally have 1000–1500 ppm of CO₂ and 4–6 wt.% H₂O; (e.g., Roggensack et al., 1997; Sisson and Bacon, 1999; Mortazavi and Sparks, 2004).

The wetting characteristics of a magma containing several mineral phases, a silicate melt and a fluid phase are complex and poorly understood. It has been shown (Navon and Lyakhovskiy, 1998) that silicate melt has a tendency to wet certain phases (e.g., feldspars), whereas the fluid preferentially wets others (e.g., Fe-Ti oxides). As feldspars are typically the most abundant mineral phase in the magmatic system of interest for this study, we use the silicate melt as the wetting phase.

Quantitative predictions were generated from the numerical solution (by the integral volume finite difference method) of partial differential equations that describe the magmatic environment. Governing equations include partial differential equations for conservation of enthalpy (see Table 1 for symbols; subscript “g” is for gas phase and “m” for silicate melt phase),

$$\begin{aligned} & \phi s_g \rho_g c_{p_g} \left(\frac{\partial T}{\partial t} + V_{D_g} \frac{\partial T}{\partial z} \right) + \phi s_m \rho_m c_{p_m} \\ & \times \left(\frac{\partial T}{\partial t} + V_{D_m} \frac{\partial T}{\partial z} \right) + (1 - \phi) \rho_{\text{xtal}} c_{p_{\text{xtal}}} \left(\frac{\partial T}{\partial t} \right) \\ & = \kappa \frac{\partial^2 T}{\partial z^2} \end{aligned} \quad (1)$$

where

$$V_{D_g} = - \frac{k_{rg}}{\mu_g} \left(\frac{\partial P_g}{\partial z} + \rho_g g \right) \quad (2)$$

and

$$V_{Dm} = -\frac{k_{rm}}{\mu_m} \left(\frac{\partial P_m}{\partial z} + \rho_m g \right) \quad (3)$$

and conservation of mass for the gas phase (H₂O–CO₂) and silicate melt,

$$\frac{\partial}{\partial t} [\phi \rho_g s_g] + V_{Dg} \frac{\partial \rho_g}{\partial z} + \rho_g \frac{\partial V_{Dg}}{\partial z} = 0 \quad (4)$$

$$\frac{\partial}{\partial t} [\phi \rho_m s_m] + V_{Dm} \frac{\partial \rho_m}{\partial z} + \rho_m \frac{\partial V_{Dm}}{\partial z} = 0. \quad (5)$$

The (total) permeability k_ϕ was calculated using the Blake–Kozeny–Carman equation (e.g., Dullien, 1979),

$$k_\phi = \frac{\phi^3 a^2}{K(1-\phi)} \quad (6)$$

where ϕ is the porosity, a the radius of the grain, and K is a constant (~ 50 – 200 for porosities > 0.1 and grain size of ≥ 0.5 mm; Rabinowicz et al., 2001; Jackson et al., 2003). On the basis of petrographic observations in silicic magmas (Best et al., 1989; Francis et al., 1989; de Silva et al., 1994; Seaman, 2000; Bachmann et al., 2002; Maughan et al., 2002), the grain size of the matrix (crystal framework) was considered to be on the order of 1–5 mm. Using this range of the grain size and porosities of 0.4–0.5, permeabilities range from 10^{-10} – 10^{-8} m².

In multiphase systems, relative saturation and relative permeability of the different phases need to be estimated. Empirical expressions are available, largely motivated by research on oil–water or water–air mixtures in porous substrates (Burdine, 1953; Millington and Quirk, 1959; Brooks and Corey, 1966; Mualem, 1976; Corey, 1977; van Genuchten, 1980; Lenhard and Parker, 1987). For the relative saturation, we used the van Genuchten function (van Genuchten, 1980):

$$s_m = \left[1 + \left(\alpha_{vg} \left[\frac{P_g - P_m}{\rho_m g} \right] \right)^n \right]^{-m} \quad \text{for } [P_g - P_m] > 0 \quad (7)$$

where

$$m = 1 - \frac{1}{n} \quad \text{and} \quad s_g = (1 - s_m)$$

with empirical constants for sandy material ($\alpha_{vg} = 0.012$ cm⁻¹, $n = 1.62$, and $m = 0.38$), and the Corey model (Corey, 1977) for the relative permeability:

$$k_{rm} = (s_m)^4 \quad (8)$$

$$k_{rg} = (1 - s_m)^2 (1 - s_m^2). \quad (9)$$

As the equations are based on experiments with water, air, and oil, we do not have the certainty that these models are perfectly applicable to a magmatic system. However, the fitting (van Genuchten) parameters in Eq. (7) (α_{vg} , n , m) are thought to scale with capillary pressure (e.g., Lenhard and Parker, 1987; Lenhard et al., 2004). We, therefore, chose van Genuchten parameters that were characteristic of sandstone and scaled them using the interfacial tension value of Bagdassarov et al. (2000). Note that the surface tension between silicic melt and fluid phase (85 mN/m) is very similar to water and air (72 mN/m). Simulations with variable values for α_{vg} , n , and m parameters were run (see Table 1 of van Genuchten, 1980 for the range of values that we used), and the results showed no significant differences.

Another potentially important aspect is the dependence of the relative permeability on the viscosity ratio of the fluid pair employed. It is certain that the viscosity ratio in the magmatic case (rhyolitic melt–hydrous fluid phase) is higher than any fluid pairs used in the water–air–oil systems. However, it has been shown (e.g., Dullien, 1979; Dullien, 1998) that the viscosity ratio has no significant influence on relative permeability when the more viscous fluid is the wetting phase (which is the case in the present study).

Constraining the possible range of porosity in silicic mushes during rejuvenation is a challenging task. Rejuvenated volcanic rocks erupt with crystal contents (~ 45 vol.%) that are slightly below the rheological transition from “rigid” porous medium to crystal-rich suspension (rheological lock-up at ~ 50 vol.% crystals; e.g., Vigneresse et al., 1996) and show evidence for some mineral dissolution, but they retain little memory of the highest crystallinity they reached. A potential approach is to measure the concentration of compatible trace elements in the glass and minerals of such magmas and estimate how much remelting of the mineral phases is required

to account for the trace element contents in the melt. For example, Fish Canyon sanidine and plagioclase, both showing textural evidence for resorption, reach concentrations of 1200 ppm for Sr_{plag} ($Sr_{\text{san}} \sim 700$ ppm) and 7500 ppm for Ba_{san} ($Ba_{\text{plag}} \sim 250$ ppm), whereas the glass contains ~ 100 ppm Sr and ~ 500 ppm Ba (Bachmann et al., 2002). With such high concentrations of Sr and Ba in the feldspars (and accounting for the dilution effect of quartz remelting), only <10 vol.% dissolution of each of these two phases (total of <20 vol.% remelting) is enough to account for the measured concentrations in the glass. Adding these 15–20 vol.% crystals to the observed 45 vol.% at eruption, one can estimate that the maximum crystallinity in the Fish Canyon may have been around 60–65 vol.%. It should be said that depletion in compatible trace elements in minerals (such as Sr in Ba in feldspars) towards the rim are known to exist (e.g., Michael, 1984), and that this zoning can lead to an underestimate of the amount of remelting as the resorbed rims of the crystals may have contained less Sr and Ba than has been measured.

In addition to the trace element budget, water and thermal budgets also suggest that *erupted* mushes never reached crystallinities higher than 70–80 vol.%. Taking into consideration that most magmas remain in the crust (plutonic/volcanic ratios are $\sim 5/1$ – $10/1$; e.g., Crisp, 1984), erupted mushes remain an exception rather than the norm. We can, therefore, envision that only the most favorable cases will lead to eruption, requiring both a high input rate of mafic magmas and the highest possible porosity to (1) reduce the heat consumed by phase change and reduce the amount of water needed to keep hydrous minerals stable, and (2) keep permeability high to allow a maximum of gas to percolate. If crystal content becomes much higher than 60 vol.%, the magma is highly likely to become a pluton, and the effect of rejuvenation will remain cryptic (although granitic bodies with evidence for thermal rejuvenation have been reported; e.g., Robinson and Miller, 1999; Miller and Miller, 2002). In this first attempt to understand gas percolation in magmatic porous media, we, thus, decided to restrain the range of porosity at 0.4–0.5.

As many magma bodies in the upper crust are sill-like, we chose to run 1-dimensional (in the vertical direction) simulations, typically with 100 vertical nodes. Numbers of grid points were varied from 10

to 1000 to test sensitivity of the discretization interval, and we determined that 100 nodes provided adequate resolution of the gradients. We acknowledge the fact that porosity (and thus permeability) in silicic mushes can vary in the horizontal dimension, and could lead to region of higher volatile (and heat) flow. However, the purpose of this study was to look at the average behavior of volatile and silicate melt flow in silicic mush using Darcy's law; 2-D simulations could have been performed, but since properties of silicic mushes are poorly known, an ad-hoc choice for the variability in porosity did not seem particularly valuable.

As finding a robust expression constraining the amount of remelting (i.e., the amount of latent heat of fusion) as a function of temperature in these water-rich, near-eutectic magmas is problematic, we decided not to explicitly include latent heat in the energy conservation equation (Eq. (1)). Instead, we decided to correct for latent heat consumption by changing the specific heat of the silicate framework. This approach provides a good approximation of the influence of latent heat on the thermal balance of system when the temperature variations are relatively small (which is the case in this study; Carslaw and Jaeger, 1959; Bergantz, 1990). We also ignored any thermodynamic effects related to exothermic reactions such as oxidation of magma (Boudreau, pers. comm.), which can be important in dry, reduced mafic magma bodies, but should not considerably perturb the heat budget in water-rich, oxidized, silicic mushes. A more complete treatment of the enthalpy balance follows in Section 5 (Discussion).

3.1. Initial and boundary conditions

At the onset of a simulation, a H_2O – CO_2 fluid phase is allowed to enter at the base of a colder porous medium saturated with high-viscosity silicate melt (with constant and homogeneous porosity). The dimensionless temperature and pressure (made dimensionless by $(P - P_{\text{UB}})/(P_{\text{LB}} - P_{\text{UB}})$, and $(T - T_{\text{mush_initial}})/(T_{\text{LB}} - T_{\text{mush_initial}})$, where subscripts UB and LB refer to “upper boundary” and “lower boundary”) were fixed at 0 for $t=0$, and the system was considered initially at lithostatic conditions. During the simulation, temperature and the pressure of the volatile phase were kept constant at the lower boundary, and pressures for both the volatile and silicate melt phase were kept

constant at the upper boundary (temperature was allowed to vary by advective outflow). The gas phase could enter and leave the system (computational domain open at both the upper and lower boundary), whereas silicate melt could exit the computational domain at the top only (no down flow in the lower boundary). A maximum value for the gas entry velocity (or volume flux per unit area; $\text{m}^3/\text{m}^2 \text{ yr}$) could be set at the lower boundary ($V_{Dg\text{max}}$), but below this maximum value, the gas flux was allowed to vary (i.e., a Dirichlet flux limited condition). In mathematical forms, these boundary conditions are:

$$P_g(0, t) = T_g(0, t) = 1 \quad (10)$$

$$P_g(z, t) = P_m(z, t) = 0 \quad \text{for } z = H \quad (11)$$

$$V_{Dm}(0, t) = 0, 0 < V_{Dg}(0, t) < V_{Dg\text{max}} \quad (12)$$

and initials conditions are:

$$T_g(z, 0) = P_g(z, 0) = P_m(z, 0) = 0 \quad (13)$$

$$V_{Dm}(z, 0) = V_{Dg}(z, 0) = 0. \quad (14)$$

4. Results

In order to assess the effect of each input parameter, we chose a standard set of values (the “primary” simulation) and ran multiple “secondary” simulations by changing one parameter at a time, holding all the others constant (i.e., parametric study). Except for gas and silicate melt fluxes, the results are all presented with dimensionless units (for T and P , see previous paragraph; time made dimensionless by a diffusive normalization; $t' = t\alpha/H^2$, where t is the time, α is the thermal diffusivity and H is the thickness of the porous medium).

The input parameters for the “primary” simulation are: (1) a ΔT ($T_{\text{final}} - T_{\text{initial}}$) of 100 °C, (2) a lithostatic pressure gradient (difference in pressure between the top and bottom boundary conditions $\Delta P = \rho g H$, where H is the thickness of the porous medium, g the acceleration due to gravity, and ρ the density of the porous medium), (3) $\text{CO}_2/\text{H}_2\text{O}$ of 0.2, (4) a permeability of 10^{-9} m^2 , (5) a viscosity of $10^{5.2} \text{ Pa s}$ (based on the viscosity of the Fish Canyon melt;

Scaillet et al., 1998), and (6) a maximum velocity for gas entering at the base of $10^4 \text{ m}^3/\text{m}^2 \text{ yr}$.

The results (Fig. 2a–c) show that the flux of gas through the system increases quickly (Fig. 2a). This relatively steady and rapid increase in hot gas flux provokes a steep rise in temperature (Fig. 2b) and decrease in the silicate melt saturation (Fig. 2c). It should be noted that at the low fluid-phase relative saturation (<1 vol.% of the pore space), the fluid phase will form individual bubbles (not a continuous network) but there is evidence that, even at fluid

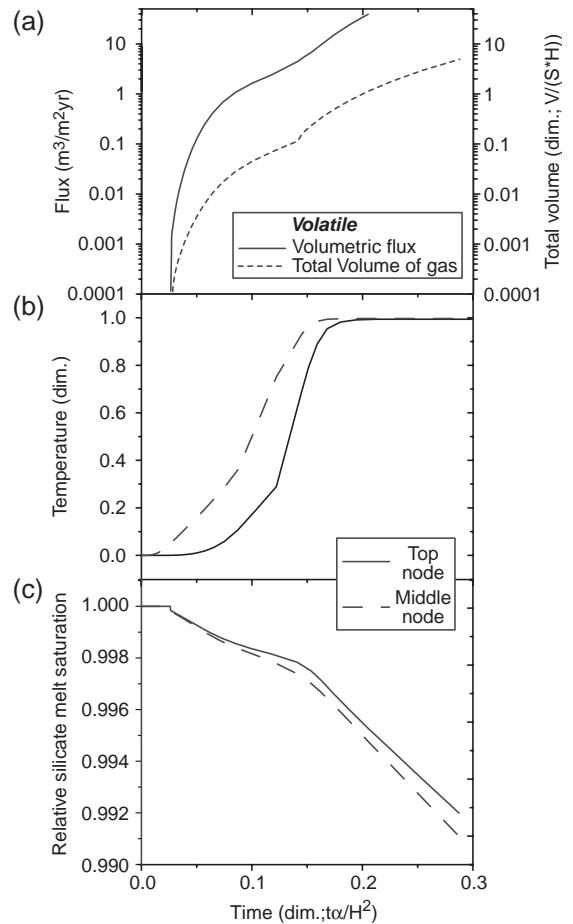


Fig. 2. Variable parameters plotted against dimensionless time. (a) Volumetric flux per unit area of gas at the bottom and top boundary and total volume of gas flowing through the porous medium (made dimensionless by dividing it by the area (S) and thickness (H) of porous medium). (b) Temperature at the middle and top node of the grid. (c) Relative silicate melt saturation at the middle and top node (gas saturation = 1 — silicate melt saturation).

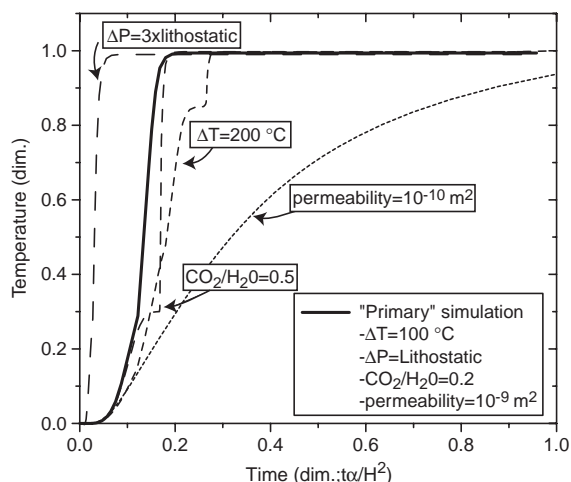


Fig. 3. Temperature variations at the top node as a function of dimensionless time for different initial and boundary conditions.

saturations < 1 vol.%, the non-wetting phase is capable of contributing to flow (Dullien, 1979).

Varying the ΔP , ΔT , $\text{CO}_2/\text{H}_2\text{O}$, permeability, and the silicate melt viscosity (keeping everything else constant) produces the following results (Figs. 3 and 4), all largely expectable from simple physical laws:

1. Increasing the pressure will increase the reheating rate of the porous medium, as the driving force for gas percolation is increased.
2. With an increasing ΔT (200 °C instead of 100 °C) and $\text{CO}_2/\text{H}_2\text{O}$ (0.2 to 0.5), the time required to reach thermal equilibrium does not change significantly. The reheating rate is slightly reduced, due to the fact that more joules need to be added for the case of a larger ΔT , and that the specific heat of CO_2 is ~ 2.5 times less than H_2O (Table 3).
3. Decreasing the porosity, and thus the permeability (assuming the grain size remains quasi-constant), slows down the reheating, as less gas can flow through the system.
4. Increasing the viscosity increases the drag on the gas phase, and decreases the reheating rate.

Small kinks appear in the curves of the flux, therefore inducing kinks in the curves of the other variables (particularly noticeable for the ΔT at 200 °C and $\text{CO}_2/\text{H}_2\text{O}$ at 0.5). Slower gas fluxes (i.e., slower Darcy velocities) are a consequence of the fact that we have tabulated the volatile densities (H_2O and

CO_2) as a function of temperature from the NIST webpage (see “Description of physical model and algorithm”), and the resulting curves are not perfectly linear, inducing slight variations in Darcy velocities. These variations are minor and do not affect the results significantly (Fig. 3).

Varying the maximum flux of gas entering the mush at the base is critical to the reheating rate by gas sparging. To assess it quantitatively, we shall consider two end-member scenarios. First, we can assume that gas is continuously available at the basal interface (i.e., rapid exsolution from the underplating more mafic magma), and that it can enter the system as fast as the porous medium allows it to (i.e. no maximum limit on the flux of gas at the lower boundary). This situation may occur for small systems and/or over fairly short periods of time, but, in the case of large volume of reheated material or for small injections of mafic magma, the supply of gas brought by the mafic reinjection will rapidly be exhausted. Therefore, the other end-member scenario involves gas fluxes averaged over long periods. An obvious lower bound is to use an average mantle-derived basalt flux in the crust, and obtain a volatile flux using some estimate of the volatile content in these magmas. Although these fluxes are subject to

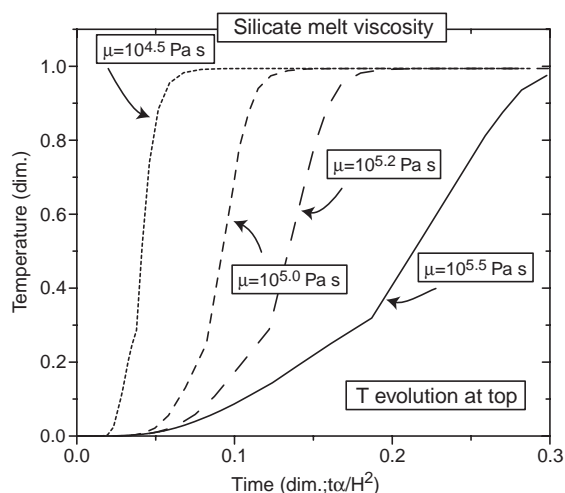


Fig. 4. Temperature variations at the top node as a function of dimensionless time for variable silicate melt viscosities. The chosen range of melt viscosity is very conservative, as our low bound ($\mu=10^{4.5}$) is the average silicic (> 70 wt.% SiO_2) melt viscosity determined by Scaillet et al. (1998).

Table 3
Material properties for the fluid phase (non wetting phase)

Parameter	Value or range	Source
Thermal conductivity (κ ; W/m K)	H ₂ O: 0.31 CO ₂ : 0.13	@ 800 °C and 270 MPa, (Lemmon et al., 2003)
Specific heat (C_p ; J/kg K)	H ₂ O: 3880 CO ₂ : 1400	@ 800 °C and 270 MPa, (Lemmon et al., 2003)
Viscosity (μ ; Pa s)	H ₂ O: 0.00007 CO ₂ : 0.00008	@ 800 °C and 270 MPa, (Assael et al., 2000) (H ₂ O) (Fenghour et al., 1998) (CO ₂)

Considered as an ideal mixture of H₂O and CO₂. κ , μ and C_p assumed constant over the chosen P – T range (600–1000 °C and 100–400 MPa).

large uncertainties, values of 50–100 km³ km⁻¹ Myr⁻¹ (volume per unit width along the strike direction of arc) appear to provide a reasonable estimate (Dimalanta et al., 2002). As volatiles never constitute more than 4–6 wt.% of the injected mafic magmas (which translates to 20–30 vol.% using densities of 2600–2800 kg/m³ for the magma and 500–600 kg/m³ for the volatile phase), volatile fluxes must range from 15–30 km³ km⁻¹ Myr⁻¹. These fluxes per arc-strike-length need to be normalized to a certain width to obtain a vertical velocity (or volumetric flux per unit area) in a case of transport in a porous medium. Typical width of volcanic provinces is on the order of 150–300 km, which give a lower bound for the flux of $\sim 10^{-3}$ – 10^{-4} m³/m² yr.

Simulations with a gas flux ranging from 10⁴ m³/m² yr (essentially unlimited) to 0 m³/m² yr show the importance of this parameter in controlling the reheat-

ing process (Fig. 5). At no or low gas flux (up to ~ 0.1 m³/m² yr), reheating occurs relatively slowly, although it remains faster than conduction (Fig. 5). This requires that, at gas flux < 0.1 m³/m² yr, heat transfer is largely conductive, although the simulations predict a slightly higher reheating rate due to some heat advection by the silicate melt (see next paragraph). When higher gas fluxes are allowed (> 0.1 m³/m² yr), the reheating rate is much faster, indicating that both the fluid and the silicate melt participate in transporting the heat.

The fact that, at no gas flux, reheating is faster than pure conduction (Fig. 5) implies that some heat is advected by the silicate melt. The simulations give exit Darcy velocities for the melt phase at the top of the system that depend on the ΔT applied between the initial temperature and the basal temperature (for $\Delta T = 100$ °C, maximum exit V_D (~ 0.001 m/yr) occur

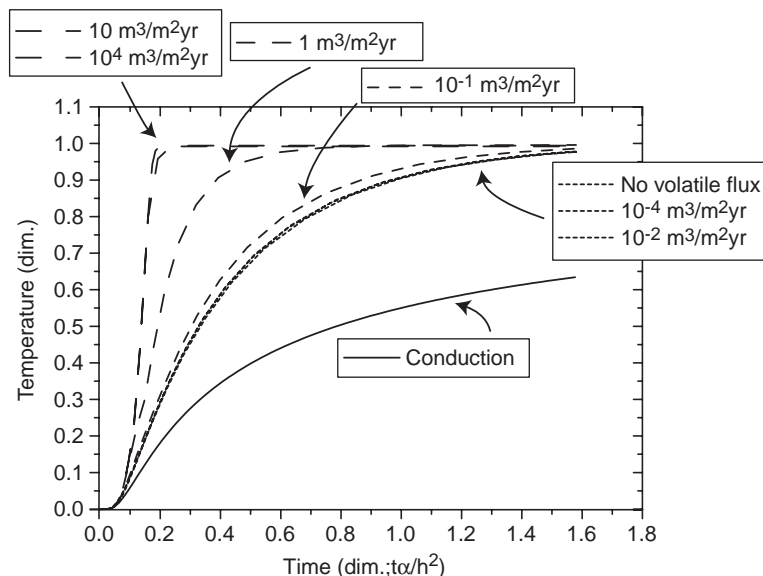


Fig. 5. Temperature variations at the top node as a function of dimensionless time for a given maximum flux of gas at the lower boundary.

immediately after the onset of a simulation and then decrease rapidly). As the Rayleigh–Darcy number ($Ra-D$) of the system ($Ra-D = (\beta_m g \rho_m C_{pm} k_\phi H \Delta T) / \mu \kappa_{xtal}$; e.g., Eq. 9–129 of Turcotte and Schubert, 2002) is always below the critical value for thermal convection in the pore space ($Ra-D = 0.005$ for $\Delta T = 100$ °C and $H = 3000$ m; $Ra-D_{critical} \geq 40$), these small exit V_D are not due to thermal convection (the thermal instability is too small to trigger convective movements) but to the differential thermal expansion between the silicate melt and crystal framework ($\beta_{melt} \gg \beta_{xtal}$). We neglect the effect of thermal expansion in the solid phase (β_{xtal} assumed to be 0), whereas the density of the silicate melt changes with temperature (using the Boussinesq approximation; $\beta_{melt} = 5 \times 10^{-5}$ 1/°K; Dobran, 2001). This differential thermal dilatation with temperature between the silicate melt and the crystalline framework leads to the expulsion of a fraction of the melt at the top of the domain. Using a $\beta_{xtal} = 0$ maximizes this effect, but some thermal advection by the differential thermal expansion of silicate melt and solids should nonetheless take place in nature as well.

At high gas fluxes, gas sparging may also play a role in driving interstitial melt out of the crystal mush due to the overpressure resulting from the forceful injection of a volatile phase in the system (see also

Anderson et al., 1984; Sisson and Bacon, 1999). As discussed by Bachmann and Bergantz (2003), this process may contribute to the generation of crystal-poor rhyolite caps in large silicic mushes but our calculation suggest that mass flux is small, most likely due to the low fluid phase saturation (≤ 1 vol.%; Fig. 2c). Fig. 6 illustrates this inefficiency, with a total amount of silicate melt expelled at the upper boundary (nondimensionalized by dividing it by the surface and thickness of the porous medium) remaining below 5% of the initial thickness of the porous medium.

5. Discussion

5.1. Application to natural examples

As mentioned in the Introduction, rejuvenated water-rich systems range in size from batholithic scale bodies (several thousands of km³) to much smaller volumes (a few km³). Using our algorithm, the gas sparging hypothesis can be evaluated by application to two well-studied systems that are end-members in terms of volume: (a) the Fish Canyon Tuff (>5000 km³), and (b) the 1995-to-present eruption of the Soufrière Hills volcano, (Montserrat, W.I.; <0.5 km³). The reason for looking at eruptions of

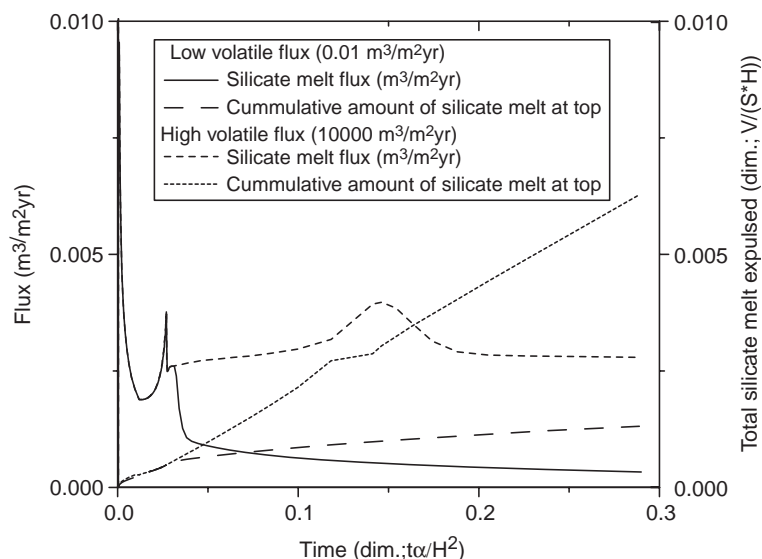


Fig. 6. Exit volumetric flux per unit area of silicate melt and total silicate melt accumulated at the top boundary (V =volume of expelled melt, S =area of porous medium, H =thickness of porous medium).

crystal mushes of widely different size is the following: for erupted volumes on the order of 1 km^3 , single injections of mafic magmas may bring enough volatiles to rejuvenate such small batches. Assuming that the exsolution of the gas phase in the mafic magma is rapid, a large volume ratio of hydrous basalt over the rejuvenated silicic mush would allow a large flux of gas into the system. In contrast, for batholithic crystal mushes, it is highly unlikely that the whole erupted volume can be rejuvenated by a single injection of hydrous mafic magma. The flux of gas (and heat) into the system should, therefore, be controlled by short-lived (compared to the lifetime of the system) high gas flux episodes (=transient sparging events) separated by periods dominated by conductive heat balance between heat loss through the roof and heat addition from below. Therefore, two diverging evolution paths could arise: (1) a fast reheating for small systems, controlled by the maximum vertical velocity of bubbles in the porous medium, and (2) a slower reheating for large systems, controlled by transient sparging events. The question of why some systems erupt small batches of magmas whereas others accumulate enormous volumes in the crust before emptying the chamber is beyond the scope of this paper, but the reader is referred to Jellinek and DePaolo (2003) for a discussion on this issue.

5.1.1. The *Montserrat andesite*

The 1995-to-present eruption of the Soufrière Hills on the island of Montserrat (W.I.) has provided the opportunity for a particularly well documented eruptive cycle (see references in Geophysical Research Letters, vol. 25, no. 18 and 19 (S.R. Young et al., eds), the Geological Society of London Memoir 21 (T.H. Druitt and B.P. Kokelaar, eds.) and the 2003 issue 44 of Journal of Petrology). On the basis of experiments coupled with zoning patterns in hornblende and Fe-Ti oxides (Devine et al., 2003; Rutherford and Devine, 2003), it appears that most of the andesite erupted from the Soufrière Hills has been reheated within ~30 days of eruption. The magnitude of the reheating is ~30 °C (from ~825 to 855 °C) and has occurred in the shallow crust (depth of ~5–6 km beneath the volcano), induced by relatively small, sill-like injections of hydrous basalt (~900–1000 °C) at the base of the andesitic magma storage region. As for all rejuvenated systems, there is scant evidence

for hybridization; heat, but little mass, has been exchanged. Currently, the favored model for the reactivation of this near-solidus magma invokes the reheating of a thin layer (~2–4 m thick) of andesitic mush by conduction at the basalt–mush interface, followed by temperature-induced self-mixing in the remobilized andesitic boundary layer once it is thick enough to undergo convection (1–2 m thick; Couch et al., 2001; Devine et al., 2003). This model assumes that the mush was able to undergo system-wide convection at all times. However, it is so crystal-rich (~50 vol.% of phenocrysts and microphenocrysts; Murphy et al., 2000) that it might have been rigid prior to the mafic reinjection. For this system, a ~30 °C reheating of a 2 m thick layer with a ΔT of 100 °C and a permeability of 10^{-9} m^2 by gas sparging is predicted to occur within 9–10 days (~10 times faster than pure heat conduction) and would require ~0.5 km^3 of gas (~2–3 km^3 of mafic magma with 4–6 wt.% volatiles, assuming an efficient gas extraction from the mafic magma). This reheating time scale is in agreement with the estimate of ≤ 30 days obtained using diffusional modeling in zoned titanomagnetite crystals (Devine et al., 2003). Whether or not the andesite mush was rigid prior to reheating, high SO_2 flux (up to 2000 tons/day; Young et al., 1998) suggests that volatiles are released from a mafic (basaltic) magma and percolate upward through the andesite mush.

5.1.2. The *Fish Canyon magma*

Using unlimited flux, reheating of 7500 km^3 of silicic mush by 40–50 °C occurs over ~20 ky, but unrealistically large volumes of gas are required (6000–8000 km^3 ; Fig. 2a), which translates into at least 20,000 to 30,000 km^3 of water-rich basalt (4–6 wt.% H_2O). On the basis of basalt flux estimates in arcs (50–100 $\text{km}^3 \text{ km}^{-1} \text{ Myr}^{-1}$; Dimalanta et al., 2002), and taking an arc segment of 100 km long (~N–S length of the caldera associated with the Fish Canyon eruption, which provides an estimate for the horizontal dimensions of the mush), a minimum of 2–3 Myr are necessary to inject enough basalt. This time period is longer than the lifespan of the Central San Juan cluster (<2 Myr; Lipman, 2000). Transient sparging events, using reasonable volumes of volatiles (200–300 km^3 of volatiles), would lead to a much longer reheating time scale (on the order of 100 ky).

Table 4
Material properties for the crystalline framework

Parameter	Value or range	Source
Thermal conductivity (κ ; W/m K)	2	(Dobran, 2001)
Specific heat (C_p ; J/kg K)	1260	(Dobran, 2001)
Density (ρ ; kg/m ³)	2890	(e.g., Whitney and Stormer, 1985)

κ , ρ and C_p assumed constant over the chosen P – T range (600–1000 °C and 100–400 MPa).

5.2. Consequence of remelting the crystal framework

As pointed out in Section 3 (Description of numerical code), the latent heat of fusion does not explicitly appear in the energy equation. To compensate for partial remelting of the crystalline framework (10–20 vol.%) on the heat budget, we modeled enthalpy exchange with an increased specific heat of the crystalline framework ($C_{p,xtal}$). We chose to double and triple the original value ($C_p = 1260$ J/kg K; Table 4) on the basis of the following calculations. The mass of mafic magma required to thermally drive the reheating of a mush of known volume by ~ 50 °C with different degrees of partial remelting can be estimated by equating the amount of sensible and latent heat released by the mafic magma ($m_{mafic}(C_{p,mafic}(T_{initial} - T_{final}) + \chi_c L_{mafic})$) with the energy needed to reheat and remelt the mush ($m_{mush}(C_{p,mush}(T_{initial} - T_{final}) + \chi_m L_{mush})$), where m is mass, C_p is specific heat, L is latent heat and χ_c and χ_m are volume fractions crystallized, respectively melted in the mafic, silicic magma. Using the following values (ΔT_{mush} of 50 °C, ΔT_{mafic} of 100 °C, χ_c of 90%, χ_m of 0%, L_{mush} of 2.7×10^5 J/kg, L_{mafic} of 4×10^5 J/kg, $C_{p,mush}$ of 1370 J/kg K and $C_{p,mafic}$ of 1484 J/kg K; Bohrsen and Spera, 2001), m_{mush}/m_{mafic} is ~ 7.4 for the case of no remelting (i.e., the minimum mass of mafic magma needed is about 15% of the mass of mush). This ratio becomes ~ 5.3 for $\chi_m = 0.1$ (i.e., for 10% remelting) and ~ 4.2 if $\chi_m = 0.2$. This suggests that $\sim 80\%$ more mafic magma (approximately twice as much enthalpy) is needed to take into consideration a 20% net remelting.

Running simulations with $C_{p,xtal} = 2 \times C_p$ (2520 J/kg K) and $3 \times C_p$ (3780 J/kg K) leads, as expected, to slower reheating rates for the cases with higher specific heat capacities. The differences are rather significant at low gas flux (10^{-2} m³/m² yr), but nearly

negligible at high flux (10^4 m³/m² yr; Fig. 7). We, therefore, submit that the effect of 20% remelting of the crystalline framework should not appreciably change our conclusions in the case of high-flux sparging. In the case of low-flux sparging, reheating time scales will be increased by a factor of 1.5 to 2.

5.3. Consequence of heat loss through roof rocks

Reheating time scales for high-flux sparging of small volumes of mush are generally too short for heat loss by conduction to the colder surroundings to be of any significance. Heat loss will only be relevant for the rejuvenation of voluminous mushes, particularly at low gas fluxes. For example, running simulations for a >5000 km³ mush with a “cooling” boundary condition at the top (Neumann condition with a heat flux of 0.1 W/m²) shows that, after 100 ky, the temperature in the middle of the mush is $\sim 25\%$ lower than without heat loss.

As mentioned in Section 3, we do not consider compaction of the matrix, which would accelerate reheating in the low-flux case due to advection of the silicate melt. Moreover, transient sparging events, also not accounted for in the timescales predicted by simulations at low gas fluxes, are likely to occur in the large systems following the emplacement of volatile-

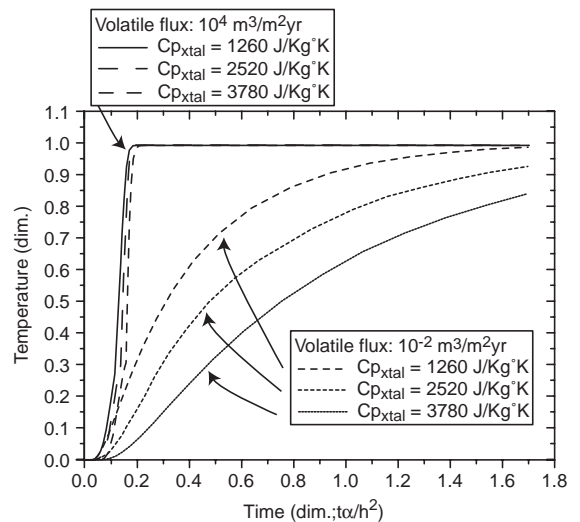


Fig. 7. Temperature variations at the top node as a function of dimensionless time for different specific heat capacities of the crystalline framework ($C_{p,xtal}$).

rich mafic magmas at the base of the mush. These short-lived (in comparison to the rejuvenation time) events can also potentially increase the reheating rate. Therefore, these two processes (compaction and transient sparging events) can partly or completely compensate for the delaying effect of heat loss through the cool roof. In summary, we stress that these simulations are helpful to show that heat advection by gas or silicate melt can transfer heat upward faster than conduction, although we concede that they provide somewhat rough estimates for the time scales of rejuvenation, particularly for the large systems.

5.4. Physical evolution of the rejuvenating mush

Our initial condition assumes that the crystals in the silicic mush form a static, rigid framework (≥ 50 vol.%). For the mush to erupt and allow for partial obliteration of the thermal gradient that develops by heat addition from below, the system has to become “liquid” again, capable of undergoing system-wide convection; the crystal framework is expected to fail as some remelting occurs. The transition from a rigid porous medium to a concentrated suspension will occur from bottom up (“unzipping” or “defrosting” of the crystal framework, (e.g., Mahood, 1990). As the Ra number is likely to reach the critical value of ~ 1000 when the boundary layer thickness is only a few meters thick, convective self-mixing (e.g., Couch et al., 2001) can occur in a small sill-like lens. This active layer propagates upward with time, leading to a crystal-rich magma that is growing in size and being progressively stirred by convection. Due to the sluggishness of the convective currents (low $Re\#$), mixing is not very efficient (mixing efficiency of < 1 ; Jellinek et al., 1999). Couch et al. (2001) have suggested a mixing efficiency of ~ 0.5 for temperature-induced self-mixing in the Montserrat andesite, and we argue that, in the scenario envisaged here, an additional convective instability can be created by the injection of a low-density gas phase from below (i.e., compositional convection), leading to a slightly higher mixing efficiency (but by no means very high). This partial mixing is in agreement with one of the most diagnostic features of these remobilized mushes (Murphy et al., 2000; Couch et al., 2001; Bachmann et al., 2002):

the absence of a noticeable thermal gradient and a homogeneous composition on a hand sample scale (10–20 cm), but not on the thin section scale.

6. Conclusion

Reheating and remobilization of near-solidus crystal mushes may be a common processes in the shallow crust and occur on large as well as small scales (Keller, 1969; Pallister et al., 1992; Nakamura, 1995; Matthews et al., 1999; Murphy et al., 2000; Bachmann et al., 2002). This recycling of the crystal-rich “leftovers” from previous magmatic episodes is linked to the injection of hot, hydrous basalt at the base of the evolved mush pile, although little hybridization may occur between the two magma types (Matthews et al., 1999; Murphy et al., 2000; Bachmann et al., 2002; Devine et al., 2003; Rutherford and Devine, 2003). The interaction seems largely constrained to heat exchange. For the Montserrat andesite, Couch et al. (2001) have proposed a model of heat exchange by conduction across the interface, followed by convective self-mixing of the overlying andesite once the critical thermal Rayleigh number is overcome. However, high crystallinity in these rejuvenated magmas can lead to the formation of a rigid skeleton, which would impede convective self-mixing to occur. A relatively fast process to advect heat vertically in rigid mushes, which remains chemically nearly invisible (cryptic chemical hybridization) and agrees with other petrological observations in erupted crystal-rich silicic systems, is to exsolve a gas phase in the hot mafic magma, and allow it to percolate upward through the silicic mush. The low viscosity and density, as well as the high specific heat of this water-rich fluid phase make it an efficient heat carrier.

Using a numerical model of two-phase flow in porous media, we have tested the likelihood of gas percolation (“gas sparging”) occurring in rigid upper-crustal silicic mushes and its potential effect on their thermal evolution. For realistic initial and boundary conditions, the heating rate will be faster than conduction. Depending on the remobilized volume, two endmember case scenarios are envisaged. For eruption of small batches of remobilized mush, such as the andesite presently produced by the Soufrière

Hills volcano (Montserrat, W.I.), single injection of hydrous basalt may contain enough volatiles to rejuvenate the whole erupted volume. In this case, flux of gas through the mush can be high ($>0.1 \text{ m}^3/\text{m}^2 \text{ yr}$; consistent with measured SO_2 fluxes at Soufrière Hills, Montserrat), and reheating occurs on the order of days to weeks. For very large volumes of rejuvenated mush, such as the Fish Canyon magma body, reheating by $\sim 50 \text{ }^\circ\text{C}$ could not be achieved by a continuous high flux sparging event as it would require geologically unrealistic amounts of hydrous mafic magmas to drive the process. In order to assess reheating rates of large systems, we ran simulations at low volatile fluxes (10^{-3} – $10^{-4} \text{ m}^3/\text{m}^2 \text{ yr}$, constrained by the average injection rate of hydrous basalt in the arc's crust). Results show that gas is not an efficient heat carrier at these low fluxes, but heating rates are still faster than conduction (Fig. 5) due to the heat advection by the silicate melt; time scales to increase the temperature of batholithic silicic mushes in the upper crust by a few tens of degrees are on the order of 100 ky.

These remobilized magmas share a common characteristic: they show no (or weak) thermal gradients and are relatively homogeneous in whole-rock composition, although they display bewildering textural and petrological complexities. They contain numerous mineral phases (up to 11 in the case of the Fish Canyon magma), many of which exhibit strong resorption textures and chemical zonation. Moreover, adjacent minerals in an erupted fragment (lava block or pumice) often display different zoning patterns. This could be a manifestation of convective self-mixing by rejuvenation at relatively low Re number prior to eruption. Couch et al. (2001) have suggested that the convection was uniquely driven by thermal instabilities. We suggest that the gas sparging hypothesis will enhance convecting self-mixing due to the coupling of two sources of density instabilities: heating and injection of a low density gas phase from the base of the system.

Acknowledgments

OB was funded by the Swiss National Science Foundation (Bourse chercheur débutant and chercheur avancé) and GWB by NSF grant EAR-0106441. We

are indebted to Mark White (PNNL, Richland, WA) for his help with the STOMP code, and to Alan Boudreau for sharing his thoughts on the thermal budgets of large magmatic bodies. Matthias Hort, Steve Sparks, Don Snyder, and three anonymous reviewers are acknowledged for their thorough reviews on previous versions of this manuscript.

References

- Allen, S.R., 2001. Reconstruction of a major caldera-forming eruption from pyroclastic deposit characteristics: Kos Plateau Tuff, eastern Aegean Sea. *Journal of Volcanology and Geothermal Research* 105, 141–162.
- Anderson, A.T., Swihart, G.H., Artioli, G., Geiger, C.A., 1984. Segregation vesicles, gas filter-pressing, and igneous differentiation. *Journal of Geology* 92, 55–72.
- Assael, M.J., et al., 2000. Experimental data for the viscosity and thermal conductivity of water and steam. *Journal of Physical and Chemical Reference Data* 29 (2), 141–166.
- Bachmann, O., Bergantz, G.W., 2003. Rejuvenation of the Fish Canyon magma body: a window into the evolution of large-volume silicic magma systems. *Geology* 31 (9), 789–792.
- Bachmann, O., Bergantz, G.W., 2004. On the origin of crystal-poor rhyolites: extracted from batholithic crystal mushes. *Journal of Petrology* 45, 1565–1582.
- Bachmann, O., Dungan, M.A., Lipman, P.W., 2002. The Fish Canyon magma body, San Juan volcanic field, Colorado: rejuvenation and eruption of an upper crustal batholith. *Journal of Petrology* 43 (8), 1469–1503.
- Bachmann, O., Dungan, M.A., Bussy, F., 2005. Insights into shallow magmatic processes in large silicic magma bodies: the trace element record in the Fish Canyon magma body, Colorado. *Contributions to Mineralogy and Petrology*. doi:10.1007/s00410-005-0653-z.
- Bagdassarov, N., Dorfman, A., Dingwell, D.B., 2000. Effect of alkalis, phosphorus, and water on the surface tension of haplogranite melt. *American Mineralogist* 85 (1), 33–40.
- Bergantz, G.W., 1990. Melt fraction diagrams: the link between chemical and transport models. In: Nicholls, J., Russell, J.K. (Eds.), *Modern Methods of Igneous Petrology: Understanding Magmatic Processes*, Reviews in Mineralogy, vol. 24. Mineralogical Society of America, pp. 240–257.
- Bergantz, G.W., Breidenthal, R.E., 2001. Non-stationary entrainment and tunneling eruptions: a dynamic link between eruption processes and magma mixing. *Geophysical Research Letters* 28 (16), 3075–3078.
- Best, M.G., Christiansen, E.H., Blank, R.H.J., 1989. Oligocene caldera complex and calc-alkaline tuffs and lavas of the Indian Peak volcanic field, Nevada and Utah. *Geological Society of America Bulletin* 101, 1076–1090.
- Bohrson, W.A., Spera, F.J., 2001. Energy-constrained open-system magmatic processes: II. Application of energy-constrained assimilation-fractional crystallization (EC-AFC) model to magmatic systems. *Journal of Petrology* 42 (5), 1019–1041.

- Brooks, R.H., Corey, A.T., 1966. Properties of porous media affecting fluid flow. *Journal of Irrigation and Drainage Division* 93, 61–88.
- Burdine, N.T., 1953. Relative permeability calculations from pore-size distribution data. *Petroleum Transactions* 198, 71–77.
- Cardoso, S.S.S., Woods, A.W., 1999. On convection in a volatile-saturated magma. *Earth and Planetary Science Letters* 168, 301–310.
- Carslaw, H.S., Jaeger, J.C., 1959. *Conduction of Heat in Solids*. Clarendon Press, Oxford.
- Corey, A.T., 1977. *Mechanics of Heterogeneous Fluids in Porous Media*, Fort Collins, Colorado.
- Couch, S., Sparks, R.S.J., Carroll, M.R., 2001. Mineral disequilibrium in lavas explained by convective self-mixing in open magma chambers. *Nature* 411, 1037–1039.
- Crisp, J.A., 1984. Rates of magma emplacement and volcanic output. *Journal of Volcanology and Geothermal Research* 20, 177–211.
- Dawson, P.B., Evans, J.R., Iyer, H.M., 1990. Teleseismic tomography of the compressional wave velocity structure beneath the Long Valley region. *Journal of Geophysical Research* 95 (B7), 11021–11050.
- de Silva, S.L., Self, S., Francis, P.W., Drake, R.E., Carlos Ramirez, R., 1994. Effusive silicic volcanism in the Central Andes: the Chao dacite and other young lavas of the Altiplano-Puna Volcanic Complex. *Journal of Geophysical Research* 99 (B9), 17805–17825.
- Devine, J.D., Rutherford, M.J., Norton, G.E., Young, S.R., 2003. Magma storage region processes inferred from geochemistry of Fe-Ti oxides in andesitic magma, Soufriere Hills volcano, Montserrat, W.I. *Journal of Petrology* 44 (8), 1375–1400.
- Dimalanta, C., Taira, A., Yumul, G.P.J., Tokuyama, H., Mochizuki, K., 2002. New rates of western Pacific island arc magmatism from seismic and gravity data. *Earth and Planetary Science Letters* 202, 105–115.
- Dobran, F., 2001. *Volcanic Processes: Mechanisms in Material Transport*. Kluwer Academics, New York, 590 pp.
- Dullien, F.A.L., 1979. *Porous Media Fluid Transport and Pore Structure*. Academic Press, New York.
- Dullien, F.A.L., 1998. Capillary effects and multiphase flow in porous media. *Journal of Porous Media* 1, 1–29.
- Eichelberger, J.C., 1980. Vesiculation of mafic magma during replenishment of silicic magma reservoirs. *Nature* 288, 446–450.
- Ewart, A., 1982. The mineralogy and petrology of Tertiary–Recent orogenic volcanic rocks: with special reference to the andesitic-basaltic compositional range. In: Thorpe, R.S. (Ed.), *Andesites: Orogenic Andesites and Related Rocks*. John Wiley, New York, pp. 25–95.
- Fenghour, A., Wakeham, W.A., Vesovic, V., 1998. The viscosity of carbon dioxide. *Journal of Physical and Chemical Reference Data* 27 (1), 31–44.
- Francis, P.W., et al., 1989. Petrology and geochemistry of the Cerro Galan caldera, northwest Argentina. *Geological Magazine* 126 (5), 515–547.
- Gauthier, P.-J., Condomines, M., 1999. ^{210}Pb – ^{226}Ra radioactive disequilibria in recent lavas and radon degassing: inferences on the magma chamber dynamics at Stromboli and Merapi volcanoes. *Earth and Planetary Science Letters* 172 (1–2), 111–126.
- Hammer, J.E., Rutherford, M.J., 2003. Petrologic indicators of preeruption magma dynamics. *Geology* 31, 79–82.
- Hildreth, W., 2004. Volcanological perspectives on Long Valley, Mammoth Mountain, and Mono Craters: several contiguous but discrete systems. *Journal of Volcanology and Geothermal Research* 136 (3–4), 169–198.
- Huppert, H.E., Sparks, R.S.J., Turner, J.S., 1982. Effects of volatiles on mixing in calc-alkaline magma systems. *Nature* 332, 554–557.
- Jackson, M.D., Cheadle, M.J., Atherton, M.P., 2003. Quantitative modelling of granitic melt generation and segregation in the continental crust. *Journal of Geophysical Research* 108 (B7), 2332.
- Jellinek, A.M., DePaolo, D.J., 2003. A model for the origin of large silicic magma chambers: precursors of caldera-forming eruptions. *Bulletin of Volcanology* 65, 363–381.
- Jellinek, A.M., Kerr, R.C., Griffiths, R.W., 1999. Mixing and compositional stratification produced by natural convection: 1. Experiments and their applications to Earth's core and mantle. *Journal of Geophysical Research* 104 (B4), 7183–7201.
- Keller, J., 1969. Origin of rhyolites by anatectic melting of granitic crustal rocks; the example of rhyolitic pumice from the island of Kos (Aegean Sea). *Bulletin Volcanologique* 33 (3), 942–959.
- Koyaguchi, T., Kaneko, K., 1999. A two-stage thermal evolution model of magmas in continental crust. *Journal of Petrology* 40 (2), 241–254.
- Koyaguchi, T., Kaneko, K., 2000. Thermal evolution of silicic magma chambers after basalt replenishment. *Transactions of the Royal Society of Edinburgh* 91, 47–60.
- Lehmann, E.W., McLinden, M.O., Friend, D.G., 2003. *Thermophysical properties of fluid systems*. NIST Chemistry WebBook, NIST Standard Reference Database Number 69 (Gaithersburg MD, 20899).
- Lenhard, R.J., Parker, J.C., 1987. A model for hysteretic constitutive relations governing multiphase flow: 2. Permeability–saturation relations. *Water Resources Research* 23, 2197–2206.
- Lenhard, R.J., Oostrom, M., Dane, J.H., 2004. A constitutive model for air–NAPL–water flow in the vadose zone accounting for immobile, non-occluded (residual) NAPL in strongly water-wet porous media. *Journal of Contaminant Hydrology* 71 (1–4), 261–282.
- Linde, A.T., Sacks, I.S., Johnston, M.J.S., Hill, D.P., Bilham, R.G., 1994. Increased pressure from rising bubbles as a mechanism for remotely triggered seismicity. *Nature* 371, 408–410.
- Lipman, P.W., 2000. The central San Juan caldera cluster: regional volcanic framework. In: Bethke, P.M., Hay, R.L. (Eds.), *Ancient Lake Creede: Its Volcano-Tectonic Setting, History of Sedimentation, and Relation of Mineralization in the Creede Mining District*. Geological Society of America Special Paper, vol. 346, pp. 9–69.
- Lipman, P.W., Dungan, M.A., Bachmann, O., 1997. Comagmatic granophyric granite in the Fish Canyon Tuff, Colorado: implications for magma-chamber processes during a large ash-flow eruption. *Geology* 25 (10), 915–918.

- Lowenstern, J.B., 2000. A review of the contrasting behavior of two magmatic volatiles: chlorine and carbon dioxide. *Journal of Geochemical Exploration* 69–70, 287–290.
- Mahood, G.A., 1990. Second reply to comment of R.S.J. Sparks, H.E. Huppert, and C.J.N. Wilson on “Evidence for long residence times of rhyolitic magma in the Long Valley magmatic system: the isotopic record in precaldera lavas of Glass Mountain”. *Earth and Planetary Science Letters* 99, 395–399.
- Marsh, B.D., 1996. Solidification fronts and magmatic evolution. *Mineralogical Magazine* 60 (1), 5–40.
- Marsh, B.D., 2002. On bimodal differentiation by solidification front instability in basaltic magmas: Part 1. Basic mechanics. *Geochimica et Cosmochimica Acta* 66 (12), 2211–2229.
- Matthews, S.J., Sparks, R.S.J., Gardeweg, M.C., 1999. The Piedras Grandes–Sancor eruptions, Lascar volcano, Chile; evolution of a zoned magma chamber in the central Andean upper crust. *Journal of Petrology* 40 (12), 1891–1919.
- Maughan, L.L., et al., 2002. The Oligocene Lund Tuff, Great Basin, USA: a very large volume monotonous intermediate. *Journal of Volcanology and Geothermal Research* 113, 129–157.
- Michael, P.J., 1984. Chemical differentiation of the Cordillera Paine granite (Southern Chile) by in situ fractional crystallization. *Contributions to Mineralogy and Petrology* 87, 179–195.
- Miller, D.S., Smith, R.B., 1999. P and S velocity structure of the Yellowstone volcanic field from local earthquake and controlled source tomography. *Journal of Geophysical Research* 104, 15105–15121.
- Miller, C.F., Miller, J.S., 2002. Contrasting stratified plutons exposed in tilt blocks, Eldorado Mountains Colorado River Rift, NV, USA. *Lithos* 61, 209–224.
- Millington, R.J., Quirk, J.P., 1959. Permeability of porous media. *Nature* 183, 387–388.
- Mortazavi, M., Sparks, R.S.J., 2004. Origin of rhyolite and rhyodacite lavas and associated mafic inclusions of Cape Akrotiri, Santorini: the role of wet basalt in generating calcalkaline silicic magmas. *Contributions to Mineralogy and Petrology* 146 (4), 397–413.
- Mualem, Y., 1976. A new model for predicting the hydraulic conductivity of unsaturated porous media. *Water Resources Research* 12, 513–522.
- Murase, T., McBirney, A.R., 1973. Properties of some common igneous rocks and their melts at high temperature. *Geological Society of America Bulletin* 84, 3563–3592.
- Murphy, M.D., Sparks, R.S.J., Barclay, J., Carroll, M.R., Brewer, T.S., 2000. Remobilization of andesitic magma by intrusion of mafic magma at the Soufrière Hills Volcano, Montserrat, West Indies. *Journal of Petrology* 41 (1), 21–42.
- Nakamura, M., 1995. Continuous mixing of crystal mush and replenished magma in the ongoing Unzen eruption. *Geology* 23 (9), 807–810.
- Navon, O., Lyakhovskiy, V., 1998. Vesiculation processes in silicic magmas. In: Gilbert, J.S., Sparks, R.S.J. (Eds.), *The Physics of Volcanic Eruptions*. Geological Society, London, pp. 27–50.
- Pallister, J.S., Hoblitt, R.P., Reyes, A.G., 1992. A basalt trigger for the 1991 eruptions of Pinatubo volcano? *Nature* 356, 426–428.
- Petford, N., 2003. Rheology of granitic magmas during ascent and emplacement. *Annual Reviews of Earth and Planetary Sciences* 31, 399–427.
- Phillips, J.C., Woods, A.W., 2002. Suppression of large-scale magma mixing by melt-volatile separation. *Earth and Planetary Science Letters* 204, 47–60.
- Philpotts, A.R., 1990. *Principles of Igneous and Metamorphic Petrology*. Prentice Hall, London, 498 pp.
- Pichavant, M., Martel, C., Bourdier, J.-L., Scaillet, B., 2002. Physical conditions, structure, and dynamics of a zoned magma chamber: Mount Pelée (Martinique, Lesser Antilles Arc). *Journal of Geophysical Research* 107 (B5). doi:10.1029/2001JB000315.
- Rabinowicz, M., Genthon, P., Ceuleneer, G., Hillairet, M., 2001. Compaction in a mantle mush with high melt concentrations and the generation of magma chambers. *Earth and Planetary Science Letters* 188 (3–4), 313–328.
- Robinson, D.M., Miller, C.F., 1999. Record of magma chamber processes preserved in accessory mineral assemblages, Aztec Wash pluton, Nevada. *American Mineralogist* 84, 1346–1353.
- Roggensack, K., Hervig, R.L., McKnight, S.B., Williams, S.N., 1997. Explosive basaltic volcanism from Cerro Negro volcano: influence of volatiles on eruptive style. *Science* 277, 1639–1642.
- Rutherford, M.J., Devine, J.D., 2003. Magmatic conditions and magma ascent as indicated by Hornblende phase equilibria and reactions in the 1995–2002 Soufrière Hills magma. *Journal of Petrology* 44 (8), 1433–1453.
- Scaillet, B., Holtz, F., Pichavant, M., 1998. Phase equilibrium constraints on the viscosity of silicic magmas: 1. Volcanic–plutonic comparison. *Journal of Geophysical Research* 103 (B11), 27257–27266.
- Schmitt, A.K., 2001. Gas-saturated crystallization and degassing in large-volume, crystal-rich dacitic magmas from the Altiplano-Puna, northern Chile. *Journal of Geophysical Research* 106 (B12), 30561–30578.
- Seaman, S.J., 2000. Crystal clusters, feldspar glomerocrysts, and magma envelopes in the Atascosa Lookout lava flow, Southern Arizona, USA: recorders of magmatic events. *Journal of Petrology* 41 (5), 693–716.
- Shimizu, A., Sumino, H., Nagao, K., Notsu, K., Mitropoulos, P., 2005. Variation in noble gas isotopic composition of gas samples from the Aegean arc, Greece. *Journal of Volcanology and Geothermal Research* 140 (4), 321–339.
- Sisson, T.W., Bacon, C.R., 1999. Gas-driven filter pressing in magmas. *Geology* 27 (7), 613–616.
- Sparks, R.S.J., et al., 1998. Magma production and growth of the lava dome of the Soufrière Hills Volcano, Montserrat, West Indies: November 1995 to December 1997. *Geophysical Research Letters* 25 (18), 3421–3424.
- Steck, L.K., et al., 1998. Crustal and mantle P wave velocity structure beneath Valles caldera, New Mexico: results from the Jemez teleseismic tomography experiment. *Journal of Geophysical Research* 103, 24301–24320.
- Stix, J., Layne, G.D., 1996. Gas saturation and evolution of volatile and light lithophile elements in the Bandelier magma chamber between two caldera-forming eruptions. *Journal of Geophysical Research* 101 (B11), 25181–25196.

- Thomas, N., Tait, S., Koyaguchi, T., 1993. Mixing of stratified liquids by the motion of gas bubbles: application to magma mixing. *Earth and Planetary Science Letters* 115, 161–175.
- Turcotte, D.L., Schubert, G., 2002. *Geodynamics*. Cambridge University Press, 456 pp.
- van Genuchten, M.T., 1980. A closed-form equation for predicting hydraulic conductivity in unsaturated soils. *Journal of the Soil Science Society of America* 44, 892–898.
- Vigneresse, J.-L., Barbey, P., Cuney, M., 1996. Rheological transitions during partial melting and crystallization with application to felsic magma segregation and transfer. *Journal of Petrology* 37 (6), 1579–1600.
- Wallace, P.J., 2001. Volcanic SO₂ emissions and the abundance and distribution of exsolved gas in magma bodies. *Journal of Volcanology and Geothermal Research* 108, 85–106.
- Wallace, P.J., Anderson, A.T., Davis, A.M., 1995. Quantification of pre-eruptive exsolved gas contents in silicic magmas. *Nature* 377, 612–615.
- Wallace, P.J., Anderson, A.T., Davis, A.M., 1999. Gradients in H₂O, CO₂, and exsolved gas in a large-volume silicic magma chamber: interpreting the record preserved in the melt inclusions from the Bishop Tuff. *Journal of Geophysical Research* 104 (B9), 20097–20122.
- Weiland, C., Steck, L.K., Dawson, P., Korneev, V., 1995. Crustal structure under Long Valley caldera from nonlinear teleseismic travel time tomography using three-dimensional ray. *Journal of Geophysical Research* 100, 20379–20390.
- White, M.D., Oostrom, M., 2000. STOMP subsurface transport over multiple phases, Version 2.0, User's guide. PNNL 12034. Pacific Northwest National Laboratory, Richland, Washington.
- Whitney, J.A., Stormer Jr., J.C., 1985. Mineralogy, petrology, and magmatic conditions from the Fish Canyon Tuff, central San Juan volcanic field, Colorado. *Journal of Petrology* 26, 726–762.
- Young, S.R., et al., 1998. Monitoring SO₂ emission at the Soufriere Hills volcano: implications for changes in eruptive conditions. *Geophysical Research Letters* 25, 3681–3684.
- Zandt, G., Leidig, M., Chmielowski, J., Baumont, D., Yuan, X., 2003. Seismic detection and characterization of the Altiplano-Puna magma body, central Andes. *Pure and Applied Geophysics* 160, 789–807.